Experimental study of the $pd \to {}^3\mathrm{He}\,K^+K^-$ and $pd \to {}^3\mathrm{He}\,\phi$ reactions close to threshold

F. Bellemann,[1] A. Berg,[1] J. Bisplinghoff,[1] G. Bohlscheid,[1] J. Ernst,[1] C. Henrich,[1] F. Hinterberger,[1] R. Ibald,[1] R. Jahn,[1] R. Joosten,[1] K. Kilian,[2] A. Kozela,[3] H. Machner,[2] A. Magiera,[4] J. Munkel,[1] P. von Neumann-Cosel,[5] P. von Rossen,[2] H. Schnitker,[1] K. Scho,[1] J. Smyrski,[4] R. Tölle,[2] and C. Wilkin[6]
(COSY-MOMO Collaboration)
[1]*Helmholtz-Institut für Strahlen-und Kernphysik der Universität Bonn, D-53115 Bonn, Germany*
[2]*Institut für Kernphysik, Forschungszentrum Jülich, D-52425 Jülich, Germany*
[3]*Institute of Nuclear Physics, Polish Academy of Sciences, Krakow, Poland*
[4]*Institute of Physics, Jagellonian University, PL-30059 Krakow, Poland*
[5]*Institut fuür Kernphysik, Technische Universität Darmstadt, D-64289 Darmstadt, Germany*
[6]*Department of Physics and Astronomy, UCL, London WC1E 6BT, United Kingdom*
(Received 28 August 2006; published 17 January 2007)

Two-kaon production in proton-deuteron collisions has been studied at three energies close to threshold using a calibrated magnetic spectrograph to measure the final ^{3}He and a vertex detector to measure the K^+K^- pair. Differential and total cross sections are presented for the production of ϕ-mesons, decaying through $\phi \to K^+K^-$, as well as for prompt K^+K^- production. The prompt production seems to follow phase space in both its differential distributions and in its energy dependence. The amplitude for the $pd \to {}^3\mathrm{He}\,\phi$ reaction varies little for excess energies below 22 MeV and the value is consistent with that obtained from a threshold measurement. The angular distribution of the K^+K^- decay pair shows that near threshold the ϕ-mesons are dominantly produced with polarization $m = 0$ along the initial proton direction. No conclusive evidence for $f_0(980)$ production is found in the data.

DOI: 10.1103/PhysRevC.75.015204 PACS number(s): 25.40.Ve, 13.60.Le, 14.40.Aq, 14.40.Cs

I. INTRODUCTION

The study of meson production in proton-nucleus collisions near threshold is of interest because of the intricate reaction mechanism that allows the momentum transfer to be shared among several nucleons and this feature becomes yet more critical as the mass of the meson is increased [1]. The simplest reaction of this type is $pd \to {}^3\mathrm{He}\,X^0$, which has the great experimental advantage that the ^{3}He can be detected in a spectrometer and the meson X^0 identified from the missing mass in the reaction. The cross sections for the near-threshold production of π^0 [2,3], η [4–6], ω [7], and η' and ϕ [8] have been extracted in this way. One drawback of this approach is, however, that in certain cases the backgrounds from multipion production can be quite large and rapidly varying. A more intrinsic problem in the case of the production of the spin-one ω and ϕ mesons is that an inclusive measurement will contain no information on their polarization. Both these difficulties can be overcome if products of the decay of the meson are detected in coincidence with the recoiling ^{3}He. The obvious solution in the ϕ case reported here is to measure the $pd \to {}^3\mathrm{He}\,(\phi \to K^+K^-)$ channel which, according to the Particle Data Group (PDG), has a 49.1% branching ratio [9]. The experiment represents an extension of our previous work, where we studied two-pion production in the $pd \to {}^3\mathrm{He}\,\pi^+\pi^-$ reaction for excess energies up to 70 MeV [10].

The basic apparatus and how it is used to identify the $pd \to {}^3\mathrm{He}\,K^+K^-$ candidates are described in Sec. II, with the method of analyzing these events obtained at three different excess energies being reported in Sec. III. The separation of ${}^3\mathrm{He}\,\phi$ events from those of prompt ${}^3\mathrm{He}\,K^+K^-$ production is based principally on the distribution in the K^+K^- invariant mass. However, it is important to demonstrate that this division is consistent with the distributions in the other kinematical variables and this is achieved in Sec. IV. The angular distributions show evidence for pure S-wave production of both prompt K^+K^- and $\phi \to K^+K^-$ pairs, with the latter being completely dominated by those where the ϕ has polarization $m = 0$ along the beam direction. Only upper limits could be placed upon the production in this reaction of the $f_0(980)$ scalar meson decaying into K^+K^-. The total cross sections for both kaon production reactions are given in Sec. V, where it is seen that the energy dependence of prompt and ϕ production seem to follow, respectively, three-body and two-body phase space. Furthermore, the amplitude for the $pd \to {}^3\mathrm{He}\,\phi$ reaction is consistent with that obtained at SATURNE using the missing-mass method [8]. Our conclusions are summarized in Sec. VI.

II. EXPERIMENT

The experiment was carried out at the MOMO (Monitor of Mesonic Observables) facility, which is installed at an external beam position of the COSY accelerator of the Forschungszentrum Jülich. Near threshold, the ^{3}He produced in the $pd \to {}^3\mathrm{He}\,K^+K^-$ reaction go into a narrow forward cone, where they can be analyzed with the high resolution 3Q2DQ spectrograph Big Karl [11]. Two sets of multiwire drift chambers (MWDC), placed in the focal plane, were used to measure the tracks of charged particles. Of these particles, the ^{3}He could be identified unambiguously using two scintillation hodoscopes, placed downstream of the MWDC and separated by 4 m, which provided energy-loss and

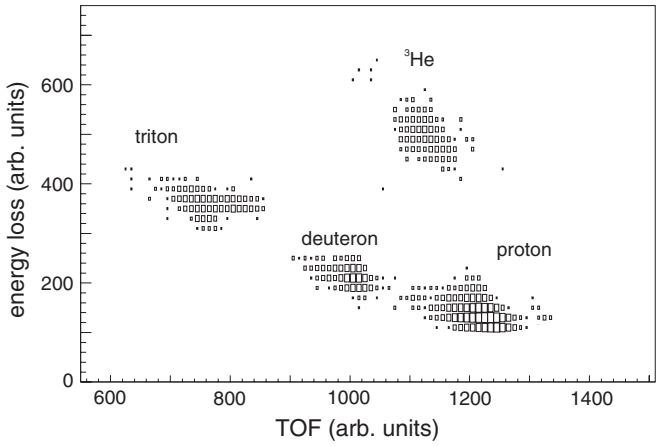

FIG. 1. Energy loss in the first scintillation layer in the focal plane of the spectrograph as a function of the time of flight between the two scintillation hodoscopes, both in arbitrary units. The well-separated groups of different particles show up very clearly.

time-of-flight information. The effectiveness of this approach is illustrated in Fig. 1, where it is seen that different particle types show up as well-separated groups.

Two charged kaons were measured in coincidence with the ^{3}He ions using the MOMO vertex detector. This combination had been proved to work successfully for two-pion production in Ref. [10]. The vertex detector, a schematic view of which is shown in Fig. 2, consists of three layers of 2.5 mm thick scintillating fibers with 224 parallel fibers in each layer. These are rotated by 60° to each other with read-outs through phototubes on opposite sides. The detector is placed outside the vacuum chamber containing the target, some 20 cm downstream of the target. Hits in three layers are required in order to avoid the combinatorial ambiguities associated with two hits.

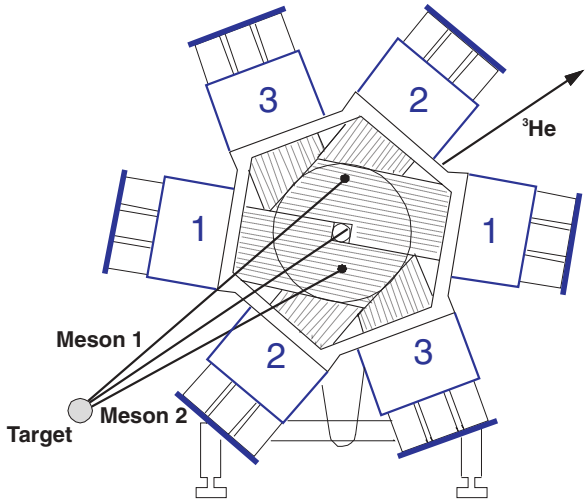

FIG. 2. (Color online) Front view to the MOMO vertex detector with the indication of a typical event. Both the primary beam and the recoil ^{3}He detected in Big Karl pass through the central hole. The numbers denote the different layers and the three boxes at the end of each read-out symbolize the phototubes. The support stand is visible in the lower part of the figure.

In contrast to the near-threshold two-pion production experiment [10], the multipion background is very large for effective masses in the GeV/c^2 region. In view of this, and in order to identify the produced particles unambiguously as kaons, the detector was supplemented by a hodoscope consisting of 16 wedge-shaped scintillators, each 2 cm thick, the details being given in Ref. [12]. This modified vertex detector was calibrated with events from elastic *pp* scattering. Charged kaons could thus be detected and their production vertex measured with full azimuthal acceptance within a polar angular range of $8^\circ < \theta_{\rm lab} < 45^\circ$. This modified vertex detector was calibrated with events from elastic *pp* scattering. It is important to note that, since there is no magnetic field associated with the MOMO detector, it is not possible to identify the charge of an individual kaon and this automatically symmetrizes some of the distributions.

The liquid deuterium target was a cylinder of diameter 6 mm and 4 mm thickness with 0.9μm mylar windows [13]. The small beam diameter of less than 2 mm led to a precise determination of the emission directions, i.e., polar and azimuthal angles. The incident beam intensity was monitored by calibrated scintillators which, on the basis of the known target areal density, allowed the absolute cross sections to be evaluated [11].

Big Karl has a momentum bite of $\pm 4\%$ of the central setting. For the central value it has a horizontal and vertical acceptance of ± 25 mrad and ± 100 mrad about the beam direction but the acceptance for the other momenta is reduced. Therefore a little above threshold all the ^{3}He from inclusive ^{3}He K^+K^- production should be covered. However, the total system is blind under such conditions since the emitted kaons fall within the central hole of the MOMO detector and are lost. On the other hand, near its threshold, the acceptance for the ϕ is high, because the transverse momentum of the ^{3}He is low while the kaon opening angle is comparatively large. It should be stressed that kaons with momenta below 160 MeV/c are stopped within the end wall of the MOMO scattering chamber so that the probability of two kaons reaching the detector is always larger than 70%.

The experiment was carried out at three overall excess energies $\varepsilon_{KK} = 35.1, 40.6$, and 55.2 MeV, i.e., excess energies in the ^{3}Heϕ system of $\varepsilon_\phi = 3.0$, 8.5, and 23.1 MeV. The restricted momentum bite of the spectrograph meant that between three and five settings of its central value were required for each beam momentum in order to provide optimal coverage of the phase space of the reaction. However, due to limited beam time, one setting was always skipped. The differential acceptances used in the subsequent analysis depended upon the particular spectrograph setting and in the construction of Fig. 3 these were weighted with the relative luminosities of the different settings. The integrated luminosity was typically 2×10^{36} cm^{-2} per setting. The differential acceptance is generally highest for the largest possible value of Q_{KK}. In such a case the kinematical ellipsoid of the ^{3}He in momentum space is the smallest so that the angular coverage of the spectrograph is then maximal. The overall acceptances achieved for the excess energies of $\varepsilon_{KK} = 35.1$ MeV,

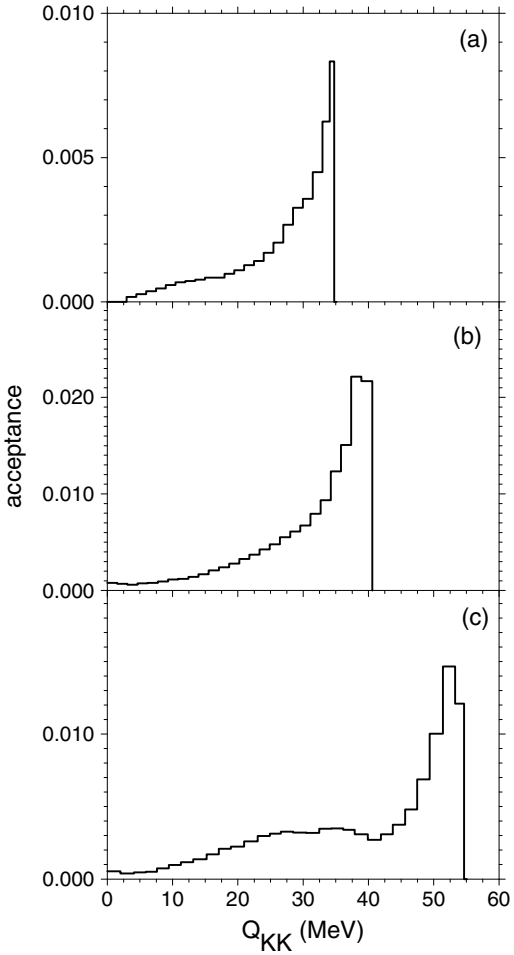

FIG. 3. Monte Carlo simulation estimates of the acceptance of the setup as a function of the excitation energy Q_{KK} at (a) $\varepsilon_{KK} =$ 35.1 MeV, (b) 40.6 MeV, and 55.2 MeV. The differing luminosities for the various spectrograph settings were taken into account.

40.6 MeV, and 55.2 MeV were about 6.9%, 21.8%, and 20.0%, respectively.

Runs were performed with an empty target cell in order to study the background. The events recorded under these conditions were analyzed in the same way as those from the target-full runs. The fraction of background events was only 0.2% and these were subtracted from the data sample.

III. DATA ANALYSIS

Having identified ${}^3\mathrm{He}\,K^+K^-$ candidates on the basis of the spectrograph and MOMO information, much of the background could be eliminated by demanding that the events be coplanar in the c.m. system. The measurement of the ^{3}He momentum together with the kaon directions means that one has a two-constraint fit to the reaction and this reduces the uncertainties in both the identification of the reaction and of its kinematics. As an example of this, we show in Fig. 4 the KK excitation energy, obtained from the missing-mass in Big Karl, plotted against that deduced from the invariant mass extracted using the reconstructed kaon momenta. Good events lie along

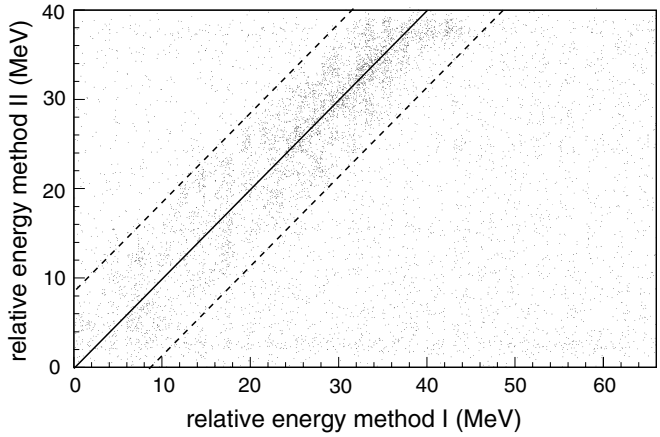

FIG. 4. The excitation energy in the KK system obtained in the $\varepsilon_{KK} = 40.6$ MeV run, evaluated I from the invariant KK mass, and II from the missing mass of the ^{3}He measured with Big Karl.

the diagonal and we retain those within $\pm 9\,\mathrm{MeV}/c^2$ of the value expected from the spectrograph measurement.

The corrections necessary for the extraction of the differential cross sections depend upon the particular angle and energy bin as well as on the spectrograph setting. The efficiency for resonant two-kaon production via the ϕ is therefore different from that of the prompt production integrated over the K^+K^- excitation energy.

The luminosity measurement needed to derive absolute cross sections has systematic uncertainties of 5% from the target thickness and 5% from the beam intensity. Another systematic uncertainty stems from the efficiency correction, which ranges from 5% up to 20% for small values of the excitation energy in the K^+K^- system. With a beam intensity of $\leqslant 10^9$ s^{-1}, the dead time was negligible. The numbers of identified events were transformed to cross sections, taking the detector efficiencies into account.

IV. DIFFERENTIAL DISTRIBUTIONS

In Figs. 5 and 6 we show the projections of the Dalitz-like plot for the $pd \rightarrow {}^3\mathrm{He}\,K^+K^-$ reaction at the three excess energies onto axes corresponding to the excitation energies Q_{KK} and $Q_{K\mathrm{He}}$ in the K^+K^- and $K\,{}^3$He systems, respectively. Since the value of Q_{KK} is fixed completely by the measurement with the high resolution spectrograph Big Karl, the distribution in this variable is the best determined of all the differential cross sections. All the other distributions rely primarily on the information furnished by the vertex detector, though the spectrograph data refines these through the kinematic fitting.

There is evidence for the production of the ϕ meson at all three energies but the physics background arising from a prompt K^+K^- production looking like phase space is very large. The distributions obtained are very different from the acceptances shown in Fig. 3 and it is important to note that the ϕ peak never falls into a region of small acceptance. The behavior of the prompt K^+K^- pairs is completely unlike that found for the $pd \rightarrow {}^3\mathrm{He}\,\pi^+\pi^-$ reaction, studied with

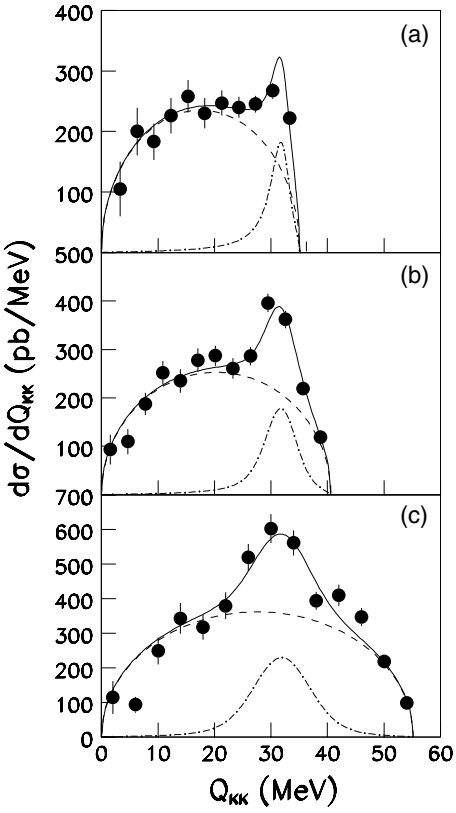

FIG. 5. Cross section for the reaction $pd \rightarrow {}^3\mathrm{He}\,K^+K^-$ as a function of the excitation energy Q_{KK} of the two kaons at overall excess energies of (a) $\varepsilon_{KK} = 35.1$ MeV, (b) 40.6 MeV, and 55.2 MeV. The events are binned in equally spaced intervals. The curves are fits to the Q_{KK} distributions in terms of phase space coming from prompt K^+K^- production (dashed line), proceeding via ϕ-meson formation (chain), and their sum (solid line).

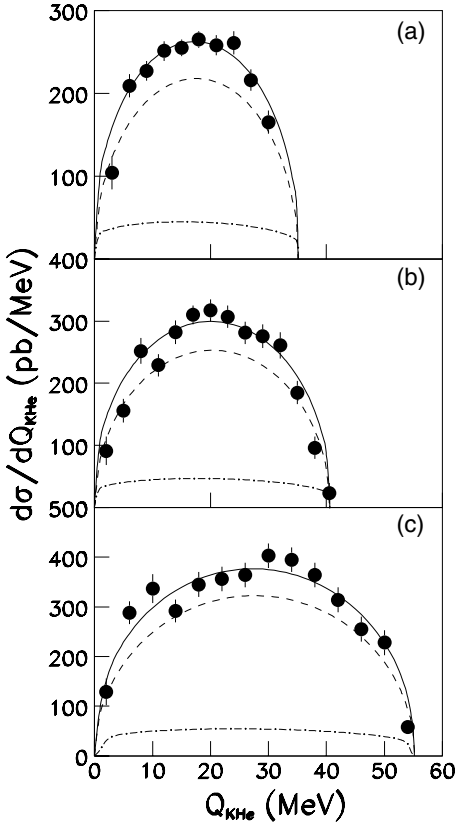

FIG. 6. Same as Fig. 5 but as a function of the excitation energy $Q_{K\mathrm{He}}$ in the $K\,{}^3\mathrm{He}$ system. The consequences of the fits shown in Fig. 5 for the $Q_{K\mathrm{He}}$ distributions are shown, though the deviations from simple three-body phase space are here relatively minor. This is due in part to the averaging over the $K^-\,{}^3\mathrm{He}$ and $K^+\,{}^3\mathrm{He}$ distributions by the MOMO apparatus.

the same apparatus [10], where effects from double p-wave production are very evident.

Fits to the excitation energy spectra have been undertaken in terms of phase space and phase space modulated by a ϕ peak, which has been taken to have a Breit-Wigner form with a natural width $\Gamma = 4.2\,\mathrm{MeV}/c^2$ [9]. This has been folded with an energy resolution width σ, which reflects uncertainties in the overall system, including the beam momentum spread, as well as effects arising from the binning of the data. The predictions of these fits are shown in Fig. 5, with their reflections on the $K\,{}^3\mathrm{He}$ spectra being presented in Fig. 6. In addition to kinematic effects, the broader ϕ peak at 55.2 MeV is due in part to the less favorable beam conditions. The general agreement achieved here supports the basic *ansatz* that the only significant distortion of phase space is that due to the ϕ peak. Though there is likely to be an effect due to the interaction of the K^- with the ^{3}He in the final state, as discussed at length in Ref. [14], its influence is minimized here by the inability to distinguish the K^- from the K^+ with the MOMO setup.

Within the present statistics, the differential cross sections for both the prompt K^+K^- and ϕ emission are independent of the ^{3}He c.m. angle, as expected for S-wave production. Figure 7 shows the variation of the cross section as a function of the opening angle between the two kaons. The phase-space distribution is expected to be about 2.2 times bigger in the backward direction than in the forward. This is a purely kinematic effect, as is the peak arising from ϕ production. The decay kaons are emitted back to back in the ϕ rest system, which coincides with the overall c.m. system at the ϕ threshold. At the lowest energy there is therefore an enhancement close to $\cos\theta_{KK} = -1$ but, for higher excess energy, this is shifted towards smaller opening angles due to the random orientation of the ϕ decay products with respect to the ϕ momentum.

Figure 8 shows the distribution in the angle between one of the kaons and the beam axis in the overall c.m. system. Pure phase-space would lead to isotropy but even the S-wave production of the ϕ meson can lead to some dependence on θ_K if the ϕ-meson is produced polarized. This can be seen more transparently in the Gottfried-Jackson frame [15], described below. This polarization effect also decreases as the beam energy is raised, because of the random orientation of the produced ϕ meson in the c.m. frame.

In the Gottfried-Jackson frame [15,16], the total momentum of the K^+K^- system is zero, which means that it is the ϕ rest frame. Since the ϕ is a vector meson, the distribution in the relative momentum of the kaons from its decay is sensitive to

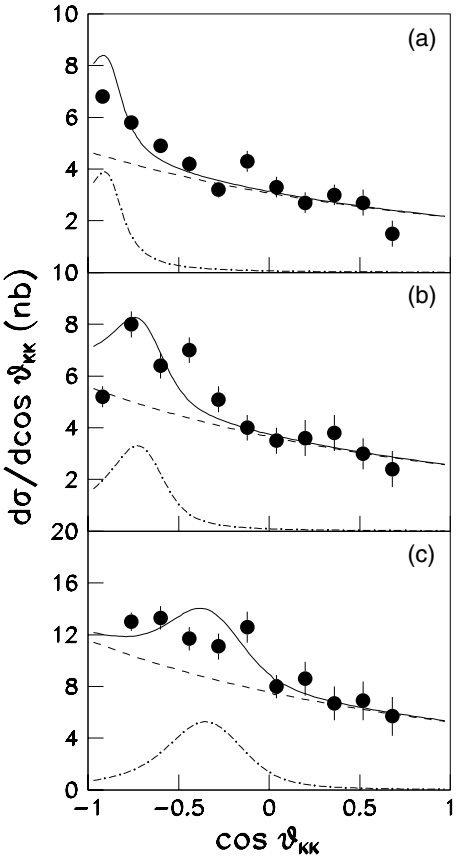

FIG. 7. Distribution in the cosine of the opening angle θ_{KK} at (a) $\varepsilon_{KK} = 35.1$ MeV, (b) 40.6 MeV, and 55.2 MeV. The dashed line represents the phase-space contribution arising from prompt K^+K^- production, whereas the chain corresponds to the ϕ component and the solid line the sum thereof.

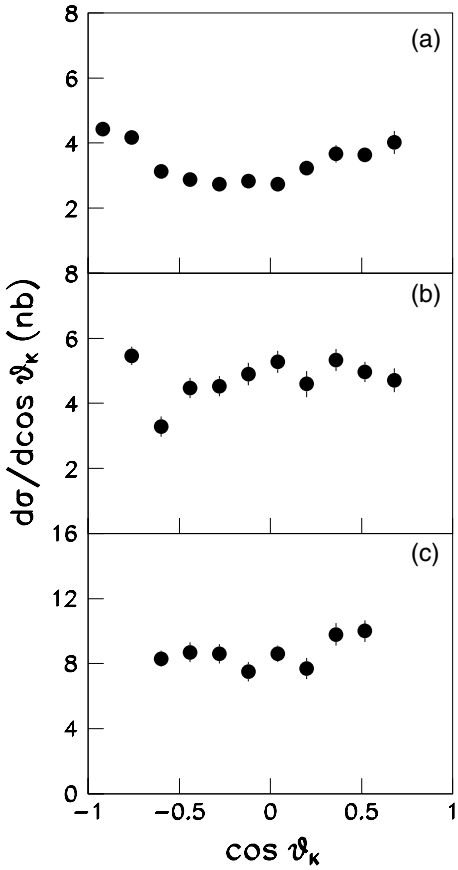

FIG. 8. Same as Fig. 7 but for the distribution in the angle between an outgoing kaon and the incident proton in the overall c.m. system. For prompt production of S-wave kaon pairs, this distribution is expected to be isotropic. However, a variation with angle can be generated through a polarization dependence of ϕ production.

its polarization with respect to some quantization axis:

$$\frac{d\sigma(\phi \rightarrow 2K)}{d\cos(\theta_{\mathrm{GJ}})} \propto \rho_{11}\sin^2\theta_{\mathrm{GJ}} + \rho_{00}\cos^2\theta_{\mathrm{GJ}}. \qquad (1)$$

Here the spin-density matrix elements ρ_{00} and ρ_{11} correspond to the populations with magnetic substate $m = 0$ and the average of $m = \pm 1$, respectively. On the other hand, the production of an S-wave K^+K^- pair would lead to a flat distribution in the decay angle θ_{GJ}.

The helicity distribution is obtained by choosing the quantization axis to lie along that of the recoiling ^{3}He nucleus. Since any anisotropy here must be proportional to the square of the ^{3}He momentum, i.e., the excess energy in the $\phi\,{}^3$He system, it is not surprising that the results shown in Fig. 9 at $\varepsilon_\phi = 3$ MeV are consistent with a flat distribution.

The axis for the Jackson angle is taken to be the relative momentum in the initial system which, for near-threshold production, can be replaced by the incident proton momentum. In the right panel of Fig. 10 the distribution in this angle is shown separately for the ϕ-rich region, where $Q_{KK} > 28$ MeV, and the remainder. In order to demonstrate the very different slopes in the two regions, the data have been arbitrarily scaled such that the cross sections have similar values when $\cos\theta_{\mathrm{GJ}} = 0$. These slopes are determined by the

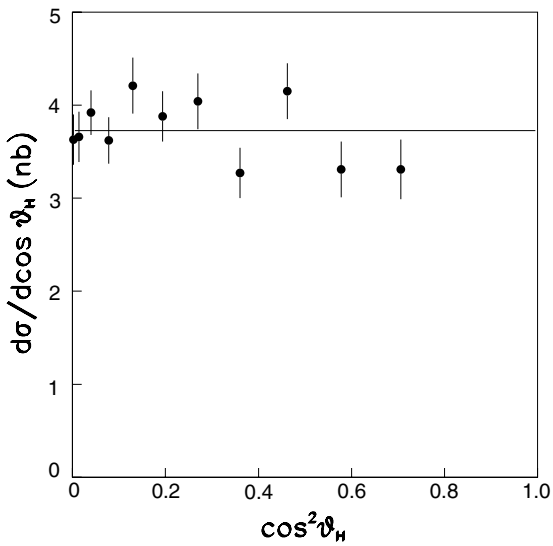

FIG. 9. Angular distributions of the kaons as a function of the helicity angle for the lowest energy of $\varepsilon_{KK} = 35.1$ MeV. The data are consistent with the average value indicated.

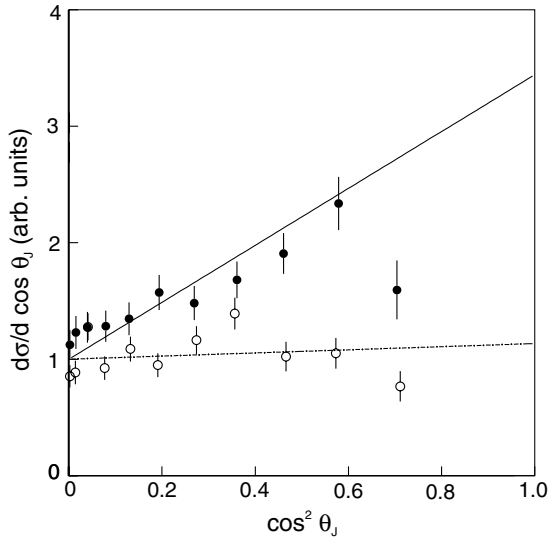

FIG. 10. Angular distributions of the kaons as a function of the Jackson angle for the lowest energy of $\varepsilon_{KK} = 35.1$ MeV. The data are divided into those with $Q_{KK} < 28$ MeV (closed circles) and $Q_{KK} > 28$ MeV (open circles). In order to show clearly the difference in slopes, the data have been arbitrarily scaled so that they have similar values at the origin. The straight lines shown here are predictions based on the fits to Fig. 5, assuming that the ϕ are produced only with $m = 0$ along the proton beam direction.

fraction of the cross section associated with ϕ production and the ϕ polarization. The straight lines in the figure are obtained by using the ϕ contribution determined from the fits to the Q_{KK} distribution of Fig. 5 assuming that the meson is produced purely with $m = 0$. This *ansatz* describes the main features of the data in both energy regions. Alternatively, fitting Eq. (1) to the data with $Q_{KK} > 28$ MeV gives $\rho_{00} = 0.82 \pm 0.05$, where the error bar is statistical and does not take into account that arising from the identification of the ϕ cross section.

The data of Fig. 5 may be used to try to put limits on the cross section for scalar meson production and, in particular, on the $f_0(980)$. Whereas PDG reports that the decay $f_0(980) \to K\bar{K}$ is merely *seen*, a recent measurement of the decay into pions and kaons performed at BES2 [17] yielded a $(25^{+11}_{-13})\%$ branch into $K\bar{K}$. We reanalyzed the Q_{KK} distribution adding incoherently a third component corresponding to a state of mass 980 MeV/c^2 and width $\Gamma = 47$ MeV/c^2. The fits yielded zero cross section for the K^+K^- branch with upper limits of 6%, 7%, and 9% of the prompt K^+K^- cross section at our three energies.

In Fig. 11 we show the shape expected for a $f_0(980)$ contribution to the differential spectrum at the three excess energies. The maximum around $Q_{KK} \approx 10$ MeV spoils the agreement with the shape of the experimental spectra. However, typically only three data points are in this range and it is precisely here that the uncertainties in the efficiency corrections are the largest. Higher statistics data would be needed to pin down unambiguously the fraction of scalar meson production in the present reaction. Such data might be obtained from studies of the stronger decay channel into two pions but the angular acceptance of the MOMO vertex detector is too small to detect these particles.

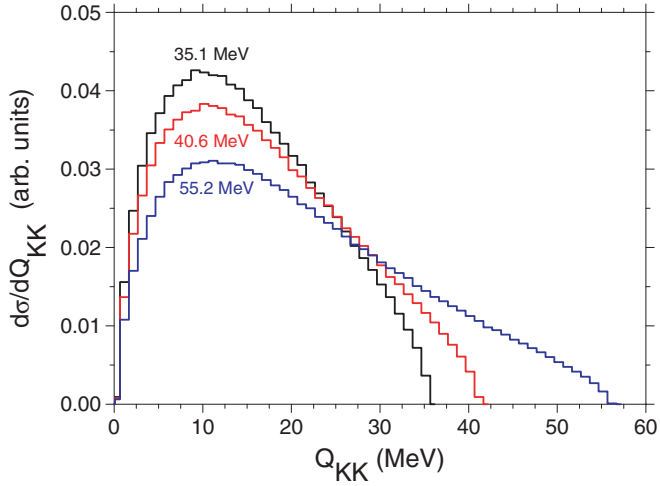

FIG. 11. (Color online) Shape of the cross section expected for the reaction $pd \to {}^3\mathrm{He}\, f_0(980)$, with the subsequent decay $f_0(980) \to K^+K^-$, for the excess energies indicated. All predictions have been normalized to unity.

V. TOTAL CROSS SECTIONS

The total ϕ and prompt kaon production cross sections, obtained by integrating the fits to Fig. 5, are presented in Table I. In the ϕ case, the branching ratio $\mathrm{BR}(\phi \to K^+K^-) = 49.1\%$ [9] has been included. The value of the energy resolution parameter σ is that deduced from the ϕ peak, after taking the natural width of 4.2 MeV/c^2 into account.

The spin-averaged square of the matrix element for ϕ production can be extracted from the total cross section using

$$|f|^2 = \frac{1}{4\pi}\,\frac{p_p}{p_{\mathrm{He}}}\,\sigma_T(pd \to {}^3\mathrm{He}\,\phi)\,, \qquad (2)$$

TABLE I. Total cross sections for prompt K^+K^- and ϕ production in terms of the incident beam momentum and their respective excess energies ε_{KK} and ε_ϕ; the ϕ results have been corrected for the 49.1% charged-kaon branching ratio. The square of the average $pd \to {}^3$He ϕ amplitude is extracted from the total ϕ production cross section through Eq. (2). In addition to the statistical errors, the quoted include also those arising from measurements of the beam intensity and uncertainties in the acceptance correction and the separation of the ϕ peak from the non resonant kaon production. Not shown is the overall uncertainty of ±5% in the areal density of the target.

Beam momentum (MeV/c)	2574 ± 1	2586 ± 1	2618 ± 2
ε_{KK} (MeV)	35.1 ± 0.5	40.6 ± 0.5	55.2 ± 0.8
σ_{KK} (nb)	6.4 ± 0.5	8.1 ± 0.5	15.8 ± 1.0
ε_ϕ (MeV)	3.0 ± 0.5	8.5 ± 0.5	23.1 ± 0.8
σ_ϕ (nb)	2.0 ± 0.4	3.0 ± 0.6	6.4 ± 1.8
$\lvert f\rvert^2$ (nb/sr)	3.0 ± 0.6	3.1 ± 0.6	3.4 ± 1.0

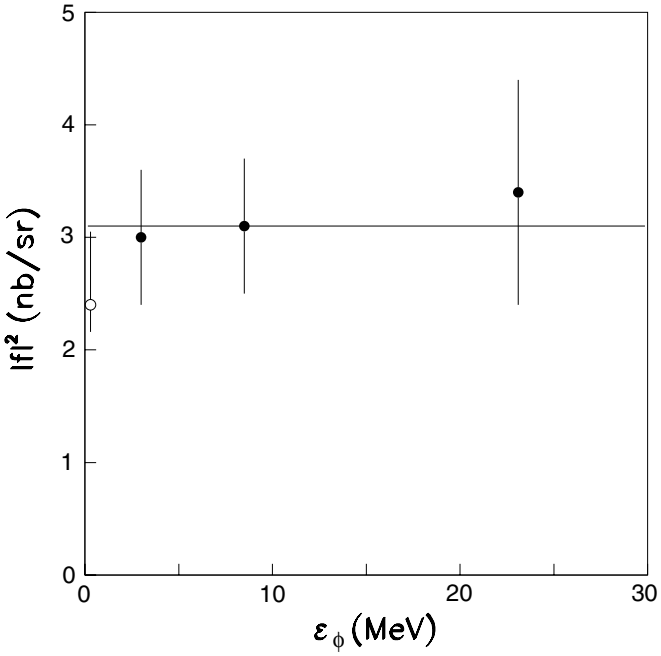

FIG. 12. The variation of the amplitude-square for ϕ production, as defined by Eq. (2), with ε_ϕ. The open circle at $\varepsilon_\phi = 0.3$ MeV is taken from the SPESIV measurement [8]. The results are all consistent with $|f|^2$ being constant, as indicated.

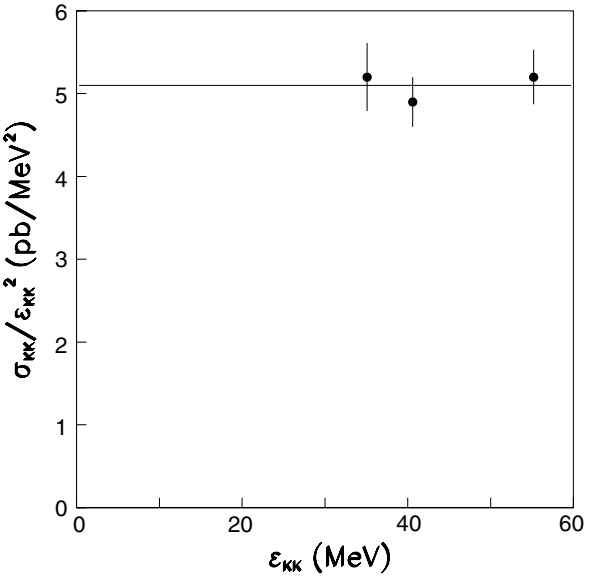

FIG. 13. Total cross section for prompt two-kaon production divided by a phase-space factor of ε_{KK}^2 as a function of ε_{KK}. The average value is also indicated.

where p_p/p_{He} is the phase-space factor of the ratio of the incident to the final c.m. momenta. Provided that there is no strong interaction between the ϕ and the ^{3}He, one would expect at these low energies to have predominantly S-wave production with very little variation of $|f|^2$, and this is what is seen from the results shown in Table I. Furthermore, the values obtained are consistent with that found with the SPESIV spectrometer [8], which at $\varepsilon_\phi = 0.3$ MeV gave $|f|^2 = (2.4 \pm 0.2\,^{+0.6}_{-0.2})$ nb/sr, where the first error is statistical and the second systematic. The mean value of this and our results, which are shown together in Fig. 12, is (3.0 ± 0.2) nb/sr. This very smooth behavior with energy is to be contrasted with the case of $pd \rightarrow {}^3\mathrm{He}\,\omega$, where the amplitude is seen to be suppressed as soon as the excess energy is similar to the width of the ω [7], though the interpretation of these data has been questioned [18].

If the prompt K^+K^- production is not influenced by resonances or other dynamical effects, then the total cross section σ_{KK} might be expected to vary like phase space, i.e., as ε_{KK}^2. The ratio $\sigma_{KK}/\varepsilon_{KK}^2$ shown in Fig. 13 is consistent with the constant value of (5.0 ± 0.2) pb/MeV^2. The absence of any obvious effects from the S-wave a_0/f_0 resonances, both in the total K^+K^- production cross sections and in the Q_{KK} distributions of Fig. 5, could be due to their very large widths and small branching ratios [9].

The ratio of ϕ to ω production in various nuclear reactions has often been discussed in terms of the Okubo-Zweig-Iizuka (OZI) rule [19], which suggests that, due to ω/ϕ mixing at the quark level, the ratio

$$R_{\phi/\omega} \equiv \frac{\sigma_T(pd \rightarrow {}^3\mathrm{He}\,\phi)}{\sigma_T(pd \rightarrow {}^3\mathrm{He}\,\omega)} \qquad (3)$$

should be of the order of $R_{\mathrm{OZI}} = 4.2 \times 10^{-3}$. As discussed by Wurzinger *et al.* [8], the difficulty in extracting numerical values for this ratio resides in the very strong and unexplained energy dependence observed in the amplitude for ω production [7]. If we follow their prescription to correct for this and other effects, we find that $R_{\phi/\omega} \approx 20 \times R_{\mathrm{OZI}}$, which is much larger than the ratio obtained in near-threshold production in proton-proton collisions at similar excitation energies [20].

For near-threshold pion production through the $pd \rightarrow {}^3\mathrm{He}\,\pi^0$ reaction, it is possible to reproduce well the experimental data [2] in impulse approximation [21], since this requires Fermi momenta in the ^{3}He nucleus only of the order of 200 MeV/c. For η production, this increases to over 400 MeV/c and other mechanisms are required to share the momentum transfer arising from the large meson mass between the nucleons. The most viable approach to describe the production of a heavy meson X seems to be within a two-step model. A pion beam is produced via $pp \rightarrow d\pi^+$ on one target nucleon, with the meson X being created through a subsequent $\pi^+ n \rightarrow p\,X$ reaction on the second nucleon in the target [22]. Though this model reproduces reasonably well the rates for η, ω, and η' production, it underpredicts ϕ production by at least a factor of five [1]. Other theoretical models are therefore necessary to describe ϕ production, possibly involving intermediate ρ as well as π mesons.

VI. CONCLUSIONS

In summary, we have made exclusive measurements of the $pd \rightarrow {}^3\mathrm{He}\,K^+K^-$ reaction at three energies above the ϕ threshold. By making fits to the K^+K^- excitation energy distribution in terms of phase space plus a resonance contribution, we have decomposed the cross section into terms corresponding to prompt K^+K^- and ϕ production.

Distributions in other variables seem to be consistent with this assumption and no firm evidence is found for the scalar resonance $f_0(980)$ decaying into K^+K^-. Both data sets are consistent with pure S-wave production, with the K^+K^- cross section varying like ε_{KK}^2 and the ϕ as $\varepsilon_\phi^{1/2}$. The most striking effect though comes from the study of the decay distribution in the ϕ rest frame, which shows that the ϕ is formed predominantly with polarization $m = 0$ along the proton beam direction, and this must be an important clue to the dynamics. Data on the analogous $pd \to {}^3\mathrm{He}\,\omega$ reaction are currently being analyzed at CELSIUS [23]. The polarization of the ω is measured through the $\omega \to \pi^0\pi^+\pi^-$ decay and the results could be particularly illuminating.

ACKNOWLEDGMENTS

The quality of the beam necessary for the success of this work is due mainly to the efforts of the COSY operator crew. Thanks goes also to Big Karl technical staff for continuous help. Support by Forschungszentrum Jülich (FFE) and Bundesministerium für Forschung und Wissenschaft is gratefully acknowledged.

[1] G. Fäldt and C. Wilkin, Phys. Lett. **B354**, 20 (1995); L. A. Kondratyuk and Yu. N. Uzikov, Phys. At. Nucl. **60**, 468 (1997).
[2] V. N. Nikulin *et al.*, Phys. Rev. C **54**, 1732 (1996).
[3] M. Betigeri *et al.*, Nucl. Phys. **A690**, 473 (2001); S. Abdel-Samad *et al.*, Phys. Lett. **B553**, 31 (2003) .
[4] J. Berger *et al.*, Phys. Rev. Lett. **61**, 919 (1988).
[5] B. Mayer *et al.*, Phys. Rev. C **53**, 2068 (1996).
[6] M. Betigeri *et al.*, Phys. Lett. **B472**, 267 (2000).
[7] R. Wurzinger *et al.*, Phys. Rev. C **51**, R443 (1995).
[8] R. Wurzinger *et al.*, Phys. Lett. **B374**, 283 (1996); R. Wurzinger, Ph.D. thesis, University of Bonn (1992); A. Kozela, Ph.D. thesis, Jagellonian University, Cracow (1994).
[9] W.-M. Yao *et al.*, J. Phys. G **33**, 1 (2006).
[10] F. Bellemann *et al.* (COSY-MOMO Collaboration), Phys. Rev. C **60**, 061002(R) (1999); F. Bellemann, Ph.D. thesis, University of Bonn (1998).
[11] M. Drochner *et al.*, Nucl. Phys. **A643**, 55 (1998).
[12] R. Ibald, Ph.D. thesis, University of Bonn (2000); J. Munkel, Ph.D. thesis, University of Bonn (2001); H. A. Schnitker, Ph.D. thesis, University of Bonn (2002).
[13] V. Jaeckle *et al.*, Nucl. Instrum. Methods A **349**, 15 (1994).
[14] V. Yu. Grishina, M. Büscher, and L. Kondratyuk, arXiv:nucl-th0608072 (2006).
[15] K. Gottfried and J. D. Jackson, Nuovo Cimento **33**, 309 (1964).
[16] E. Byckling and K. Kajantie, *Particle Kinematics* (Wiley, NY, 1973).
[17] M. Ablikim *et al.*, Phys. Lett. **B607**, 243 (2005).
[18] C. Hanhart and A. Kudryavtsev, Eur. Phys. J. A **6**, 325 (1999).
[19] S. Okubo, Phys. Lett. **5**, 165 (1963); G. Zweig, CERN report TH-401 (1964); I. Iizuka, Prog. Theor. Phys. Suppl. **37**, 21 (1966).
[20] M. Hartmann *et al.*, Phys. Rev. Lett. **96**, 242301 (2006).
[21] J.-F. Germond and C. Wilkin, J. Phys. G **16**, 381 (1990).
[22] K. Kilian and H. Nann, AIP Conf. Proc. **221**, 185 (1990).
[23] K. Schönning and B. Höistad (private communication).